frontiers in Earth Science

ORIGINAL RESEARCH
published: 16 June 2021
doi: 10.3389/feart.2021.609321

Water Vapor Changes Affect Cross-Seasonal Strong Drought Events in the Eastern Region of Northwest China

Yu Zhang[1], *Kang Liu*[2]*, *Yaohui Li*[1,3], *Wei Shen*[4], *Yulong Ren*[1], *Dingwen Zeng*[1] *and Sha Sha*[1]

[1]*Key Laboratory of Arid Climate Change and Disaster Reduction of CMA, Key Laboratory of Arid Climatic Change and Reducing Disaster of Gansu Province, Institute of Arid Meteorology, Lanzhou, China,* [2]*Gansu Provincial Meteorological Service Center, Lanzhou, China,* [3]*Civil Aviation Flight University of China, Guanghan, China,* [4]*Suqian Meteorological Bureau, Suqian, China*

OPEN ACCESS

Edited by:
Zhiwei Zhu,
Nanjing University of Information Science and Technology, China

Reviewed by:
Jiali Wang,
Argonne National Laboratory (DOE), United States
Wenting Hu,
Institute of Atmospheric Physics, Chinese Academy of Sciences (CAS), China

***Correspondence:**
Kang Liu
kang_liu1984@163.com

Specialty section:
This article was submitted to Atmospheric Science, a section of the journal Frontiers in Earth Science

Received: *23 September 2020*
Accepted: *27 May 2021*
Published: *16 June 2021*

Citation:
Zhang Y, Liu K, Li Y, Shen W, Ren Y, Zeng D and Sha S (2021) Water Vapor Changes Affect Cross-Seasonal Strong Drought Events in the Eastern Region of Northwest China. Front. Earth Sci. 9:609321. doi: 10.3389/feart.2021.609321

Drought in eastern Northwest China (ENC) is severely affected by water vapor conditions. An in-depth study of the primary sources of water vapor and its characteristics, at intraseasonal and interannual timescales, was conducted. This information is crucial for further study of the causes and mechanisms of extreme droughts and floods in the ENC. This study evaluated the spatial distribution and transport characteristics of water vapor over ENC during the 1981–2019 period based on the fifth generation of the European Center for Medium-Range Weather Forecasts atmospheric reanalyzes data of the global climate (ERA5). We studied the water vapor transport routes, water vapor convergence, water vapor budgets as well as the changes in water vapor fluxes and budgets over time in four areas surrounding ENC. The Mediterranean Sea, Black Sea, Caspian Sea, Indian Ocean, Bay of Bengal, and the South China Sea were the main sources of water vapor in ENC, supplemented by mid to high-latitude continental sources. The monthly change in water vapor flux in ENC exhibited the peak on July. The transport of water vapor in ENC was mainly toward the east and north. For most cross-seasonal drought events, the water vapor output is the main way in the south boundary and the west boundary. However, for the longest duration of cross-seasonal strong drought events, it is characterized by that the water vapor output is the main way in the south boundary, while the water vapor input in the north boundary is obviously weak. Water vapor paths in cross-seasonal strong drought events are analyzed, by which the Hybrid Single-Particle Lagrangian Integrated Trajectory model (HYSPLIT). The intensity of the subtropical high in the western Pacific is weak and the position is south, which corresponds to the occurrence of cross-seasonal strong drought in the ENC.

Keywords: water vapor source, water vapor budget, water vapor transport routes, water vapor convergence, eastern region of northwest China, cross-seasonal strong drought events

Abbreviations: ENC, eastern Northwest China; NWC, northwestern China.

INTRODUCTION

The ENC is located on the northeastern side of the Qinghai-Tibet Plateau, including the 30–40°N, 100–110°E area in China. This region has a temperate mainland climate and is affected by summer monsoons, and the precipitation variability is large (Sun, 1997). In the past half century, the eastern part of Northwest China has experienced a trend of warm drying, especially after the 1970s (Zhang et al., 2003). However, precipitation in the eastern part of Northwest China changed from decreasing to increasing in the early 21st century (Ma et al., 2020). When the East Asian summer monsoon is affected by peripheral airflow and the plateau topography of the western extension subtropical high, droughts and floods in the eastern part of the Northwestern region will be affected by the water vapor transport of the East Asian monsoon (Qian et al., 2018). The action of plateau geomorphism results in the ENC functioning as a "gateway" for the warm and wet ocean current to enter the northwestern inland area, which is the key area to maintain air–water sources and even the water circulation process in the northwestern inland area (Ren et al., 2004).

Water vapor transport is a key link in the water circulation process, especially atmospheric water sources. Climate studies have determined the characteristics of water vapor transport and water vapor budgets over land. Researchers have also evaluated the distribution of water and gas resources and the characteristics of movement over watersheds. For example, Roads et al. (1994), Ninomiya (1999), and Bisselink and Dolman (2008) used reanalysis data to explore the relationship between water vapor transport and the water cycle in North America, Europe, Asia, and Australia. They obtained the following results from studies in different regions: Precipitation anomalies were approximately equal to atmospheric moisture flux convergence anomalies. Liu and Stewart (2003) and Draper and Mills (2008) found a significant difference in water vapor transport between the meridional and latitudinal directions by studying the water vapor transport characteristics of watersheds in North America and Australia, which is the direction of the meridional moisture fluxes changes with seasons, but that of the zonal moisture fluxes does not. Arraut and Satyamurty (2009) studied the characteristics of winter precipitation and tropospheric water vapor transport in the Southern Hemisphere. They found that on the South American continent, precipitation was highly correlated with water vapor transport, while the correlation coefficient was lower for the ocean. Knippertz and Wernli (2010) documented the impact of strong water vapor output in summer in tropical regions. The influence of the components of some monsoon systems on airborne water sources has also been studied. Kwon et al. (2005) analyzed the connection with the Indian monsoon. Muñoz et al. (2008) demonstrated the relationship between the precipitation and convergence/divergence of water vapor flux in low-level jets by studying low-level jets in the Caribbean during summer. The strongest characteristics of low-level jets occurred from May to September Sohn and Park (2010) showed the effects of Hadley circulation and Walker circulation on water vapor transport. According to Perdigón-Morales et al. (2020), the main moisture sources for modulating the midsummer drought region in Mexico during summer were identified using the Lagrangian particle dispersion model on the Flexible Particle Dispersion Model (FLEXPART) for the 1979–2017 period. From this analysis, the Caribbean Sea was identified as one of the main moisture sources. Dai and Wang, (2020) pointed out that the seasonal distribution of precipitation in the arid region of central Asia is related to the meridional component of local water vapor transport, and the seasonal water vapor transport is accompanied by water vapor convergence/divergence to the north/south, corresponding to the high/low seasonal precipitation ratio. Most of central Asia is characterized by water vapor divergence in spring and summer and by water vapor convergence in winter. In the arid region of China, input of water vapor occurs mainly along the western and northern boundaries, whereas output occurs along the eastern boundary and remains largely constant in autumn and summer (Guan et al., 2019).

Under global warming (especially in recent decades), the precipitation increase and the climate humidification trend in the arid region of Northwest China (NWC) are important scientific issues that have attracted academic attention (Chen et al., 2019). Ren et al. (2016) pointed out that since 1979, in the arid region of NWC, there has been a significant increase in the whole-layer integral water vapor flux, which is mainly due to a significant decrease in the output flux of the eastern boundary rather than an increase in the input flux of the western, southern, and northern boundaries. Peng and Zhou (2017) argued that, from a thermodynamic point of view, the increase in precipitation is related to the increase in local evapotranspiration, while from a kinetic point of view, the southward shift of the westerly belt leads to an increase in precipitation due to the abnormal convergence of water vapor over the northwest. The climate in the arid region of NWC is mainly controlled by westerly circulation, predominantly summer precipitation, and the annual water vapor is mainly derived from westerly transport at mid-latitudes (Zhang et al., 2019). The extreme western extension of the western Pacific subtropical high can also strengthen the high ridge above the Mongolian plateau and strengthen the divergence over the Mongolian plateau. Anti-cyclone activity on the Mongolian Plateau contributes to the westward transport of water vapor, resulting in an increase in precipitation in the arid region of the Northwest (Chen F et al., 2021). In recent years, academic circles have gained a new understanding of the mechanism of summer precipitation increase in NWC's arid region, but there are great differences in sources (Wu et al., 2019). Chen C et al. (2021) showed that there is no obvious prevailing wind direction in the northern part of the Qinghai-Tibet Plateau in summer. Therefore, it is necessary to use seasonal average water vapor to study water vapor transport in northwestern arid regions. If the water vapor transport of extreme precipitation in northwestern arid regions is ignored, the contribution of local evaporation to precipitation change in northwestern arid regions may be exaggerated.

Since the beginning of the 21st century, some scholars have called for strengthening of the analysis of water vapor transport in the arid region of NWC, but the study of water vapor in the ENC mainly focuses on wet events. However, dry events are rarely

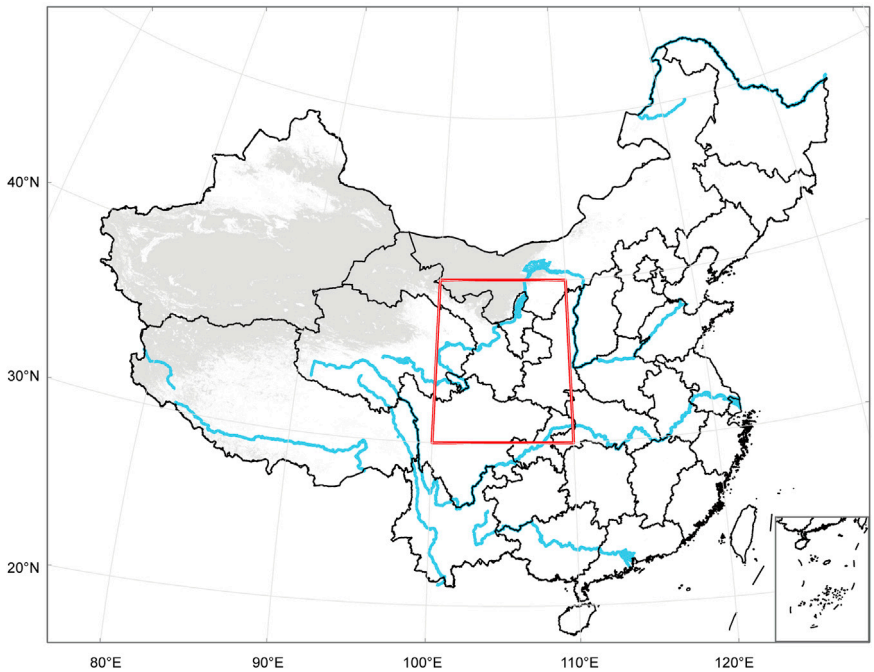

FIGURE 1 | The range of the eastern region of eastern Northwest China.

analyzed in terms of water vapor source and transport. Relatively few other studies have been conducted on water vapor transport in this region. Airborne water sources are not only seasonal features but also important processes that exist throughout the year and constitute the water cycle in the region. Cross-seasonal drought in the north is frequent, long, and intense, and more importantly, the impact of seasonal persistent drought on agricultural production, ecological improvement, and water source replenishment in the above areas is more serious than that caused by a single seasonal drought (Yang et al., 2013). Therefore, it is important to study the main sources of water vapor in the ENC as well as the variation in extreme drought events. In this paper, we aim to understand the cause of droughts and floods in the ENC by studying the characteristics of water vapor in the whole year and the characteristics of water vapor transport during extreme drought events.

DATA AND METHODS

Data

In this paper, ERA5 daily and monthly data (0.25° × 0.25° latitude and longitude) from 1981 to 2019 were used. The elements used include the specific humidity in each layer from 1,000 hPa to 100 hPa, u-wind, and v-wind. And sea surface temperature (SST). The scope of the eastern part of ENC is based on previous research results. The ENC is outlined by the rectangular range (30–40°N, 100–110°E) shown in **Figure 1**.

Methods

(1) Water vapor flux and water vapor flux divergence

Assuming that there is less water vapor in the atmosphere above 300 hPa, the entire water vapor transport flux $Q = (Q_\lambda, Q_\varphi)$ per unit gas column can be calculated by the following formulas.

$$Q_\lambda = \frac{1}{g}\int_{300}^{P_s} uqdp, \tag{1}$$

$$Q_\phi = \frac{1}{g}\int_{300}^{P_s} vqdp. \tag{2}$$

We determined the water vapor flux of each grid point. Then, the water vapor fluxes of all grid points in the study area were averaged to provide a measure of the water vapor flux in the area.

(2) Water vapor balance along each boundary was calculated as follows:

$$F_\lambda = \int_{y_1}^{y_2} Q_\lambda dy, \tag{3}$$

$$F_\phi = \int_{x_1}^{x_2} Q_\phi dx. \tag{4}$$

If $F_\lambda > 0$, water vapor is transported eastward; if $F_\lambda < 0$, water vapor is transported westward. If $F\varphi > 0$, water vapor is transported northward; if $F\varphi < 0$, water vapor is transported southward. When $F > 0$, water vapor is considered water vapor input, when $F < 0$, water vapor is considered water vapor output.

(3) Water vapor flux divergence

In the spherical coordinate system, the divergence of water vapor transport flux in a certain area can be calculated by the following formula.

$$\nabla \cdot Q = \frac{1}{a\cos\varphi}\left(\frac{\partial Q_\lambda}{\partial \lambda} + \frac{\partial Q_\varphi \cos\varphi}{\partial \varphi}\right),$$

$\nabla \cdot Q > 0$, indicates water vapor divergence; $\nabla \cdot Q < 0$, indicates water vapor convergence.

(3) Cross-Seasonal Strong Drought Events

Atmospheric drought is studied in this paper, and the cross-seasonal drought events are based on the CI.

(4) HYSPLIT

In this paper, the Lagrangian model on Hybrid Single-Particle Lagrangian Integrated Trajectory model (HYSPLIT) driven by ERA5 data was used to analyze the moisture transport track and the track of the different grades of the cross-seasonal strong drought events in the ENC. The HYSPLIT model is a complete system for computing simple air parcel trajectories, as well as complex transport, dispersion, chemical transformation, and deposition simulations. HYSPLIT continues to be one of the most extensively used atmospheric transport and dispersion models in the atmospheric sciences community. A common application is a back trajectory analysis to determine the origin of air masses and establish source-receptor relationships.

ANALYSIS OF WATER VAPOR FACTORS AFFECTING EXTREME DROUGHT EVENTS

Water Vapor Source

The monthly average vapor flux (**Figure 2**) shows that from December to February, an anticyclonic circulation exists in the Mediterranean Sea, Black Sea and the Caspian Sea. The maximum of water vapor flux can exceed 50 g cm^{-1} hPa^{-1} s^{-1}. The westerlies to the east of the anticyclonic circulation are blocked by the western part of the Qinghai-Tibet Plateau, which affect the upper-layer circulation over the plateau. The upper-layer airflow over the plateau further influence the circulation in the ENC. Due to the long distance traveled and the ascent, the water vapor flux is less than 50 $gcm^{-1}{\cdot}hPa^{-1}{\cdot}s^{-1}$ by the time it reaches ENC. From December to February, the anticyclonic circulation exists under a stable state and it is the main source of water vapor in ENC. Compared to winter, the flow field form changes little from March to April, but the curvature of the streamline over the Qinghai-Tibet Plateau decreases. This indicates that the water vapor reaching the eastern part of the NWC increases slightly. Additionally, there are large-value centers with water vapor fluxes exceeding 100 $g{\cdot}cm^{-1}{\cdot}hPa^{-1}{\cdot}s^{-1}$ in the Bay of Bengal and the Indian Peninsula. The anticyclonic circulation in the western Pacific `moves slightly northward, and it reaches the ENC under the westerly airflow. At this time, the water transport of the western Pacific Ocean is lifted to the north than last month and the water vapor of Indian Ocean transported to the ENC. Convergence has been formed at Indian Ocean April. In May, the flow field is adjusted more complex than that in March and April. The anticyclonic circulation in the Arabian Sea and the Mediterranean Sea has disappeared. And this phenomenon has been replaced, by which the westward flow is diverted to the east and south. At the same time, large-value centers of a water vapor flux greater than 100 $g{\cdot}cm^{-1}{\cdot}hPa^{-1}{\cdot}s^{-1}$ appear near the Indian peninsula in the Arabian Sea. Further, there is a trough in the eastern part of the Indian peninsula, and there is a southwesterly airflow in front of the trough transporting water vapor to the east of the midwest regions. Another important feature in May is the increase in water vapor flux in the mid to high latitudes of Asia, which is transported by the northwesterly airstream to the ENC.

From June to August, there are three water vapor channels in the ENC. The main water vapor channel is from the Indian Ocean and the Bay of Bengal. The water vapor channel flows northward through Tibet and the Sichuan Basin to the ENC. The second channel is from the western Pacific Ocean and is transported northward by the Indian Ocean monsoon to the ENC. The third channel is from the northwesterly flow of the mid- and high latitudes. In August, these three channels of water vapor converge and benefit the generation of the rainy season in ENC.

The water vapor in the ENC is mainly derived from the Bay of Bengal and the South China Sea in September. The water vapor is transported by the Indian monsoon and subtropical high circulation to the ENC forming a convergence. In October, the water vapor in the Indian Ocean decreases. The water vapor mainly originates from the South China Sea and is transported by subtropical high pressure to the ENC. There is also a relatively weak water vapor transport by the northwest airflow to the ENC. The water vapor from the Indian Ocean and the subtropical high is disappeared in November, and the main water vapor source is the Arabian Peninsula.

This analysis shows that the water vapor in the ENC derives mainly from the Mediterranean Sea, Black Sea, Caspian Sea, Indian Ocean, Bay of Bengal, South China Sea, and the mid-high latitude continent. From December to March, the water vapor is mainly transported from the Mediterranean Sea, Black Sea, Caspian Sea, and Indian Ocean, supplemented by water vapor transport in the mid- and high latitudes. From September to November, the Bay of Bengal and the South China Sea are most important for water transport. From June to August, all four water vapor sources contribute to the convergence in the ENC.

The average water vapor flux in ENC (**Figure 3**) shows that from December to February, the water vapor in the ENC is mainly transported to the east, and the turbulent water vapor flux is small. In January and February, the zonal water vapor transport increases slightly, and the zonal water vapor flux in the south of Gansu and Shanxi provinces is 40 $g{\cdot}cm^{-1}{\cdot}hPa^{-1}{\cdot}s^{-1}$. In the spring, the zonal water vapor transport in the ENC is dominated by weak eastward transport, with relatively high eastward transport in March In summer, the zonal transport of water vapor in the ENC is mainly eastward, but the water vapor transport in the central part of Gansu, northern Ningxia and northern Shanxi is negative, indicating that there is a weak westward transport of water vapor. The ENC is in the convergence area of the east-west water vapor

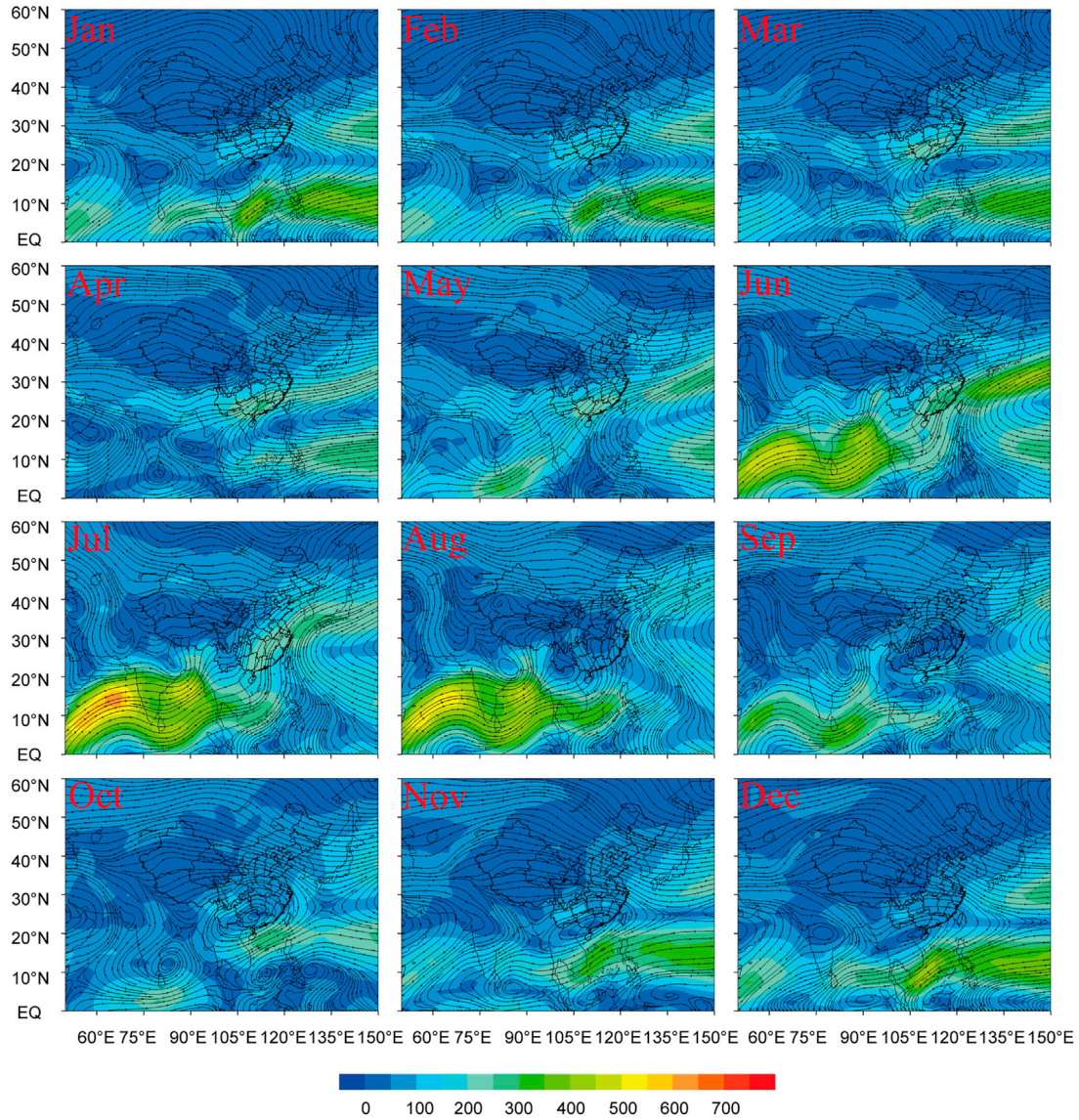

FIGURE 2 | The monthly average vapor flux (Unit: $gcm^{-1}{\cdot}hPa^{-1}{\cdot}s^{-1}$).

transport. From September to November, the zonal water vapor transport is still mainly eastward. The zonal water vapor flux in September is relatively high. The water vapor is the smallest in November, corresponding to the period of lowest precipitation in the eastern part of the western region.

The monthly change in the water vapor flux in the ENC is parabolic. Overall, the change within a year shows two peaks. In Jan., the water vapor flux is 34.12 $g{\cdot}cm^{-1}{\cdot}hPa^{-1}{\cdot}s^{-1}$, after which the water vapor flux gradually increases. In Jun., the water vapor flux increases rapidly to 60 $g{\cdot}cm^{-1}{\cdot}hPa^{-1}{\cdot}s^{-1}$. However, there is a dramatic reduction in the August. Then, the water vapor flux increases again to reach the highest value in Sep., i.e., 64.21 $g{\cdot}cm^{-1}{\cdot}hPa^{-1}{\cdot}s^{-1}$. The water vapor flux is the smallest in Jan., i.e., 34.12 $g{\cdot}cm^{-1}{\cdot}hPa^{-1}{\cdot}s^{-1}$. The meridional water vapor flux for the entire year (January–December) in the ENC is weakly positive, indicating that the water vapor is mainly transported northward.

Based on the above analysis, the water vapor in the ENC is mainly transported to the north and east. Water vapor is high during the main rainy season (June–August) but relatively low in the other seasons.

Water Vapor Convergence

The monthly water vapor flux divergence (**Figure 4**) shows that the ENC is largely in the weak water vapor convergence zone in winter, but the water vapor gradually increases over time. By March, the water vapor flux divergence reaches $-0.5\ g{\cdot}cm^{-2}{\cdot}hPa^{-1}{\cdot}s^{-1}$. The water vapor convergence center is located at the junction of Sichuan, Gansu and Shanxi provinces. Compared with the winter, the position of the negative area of

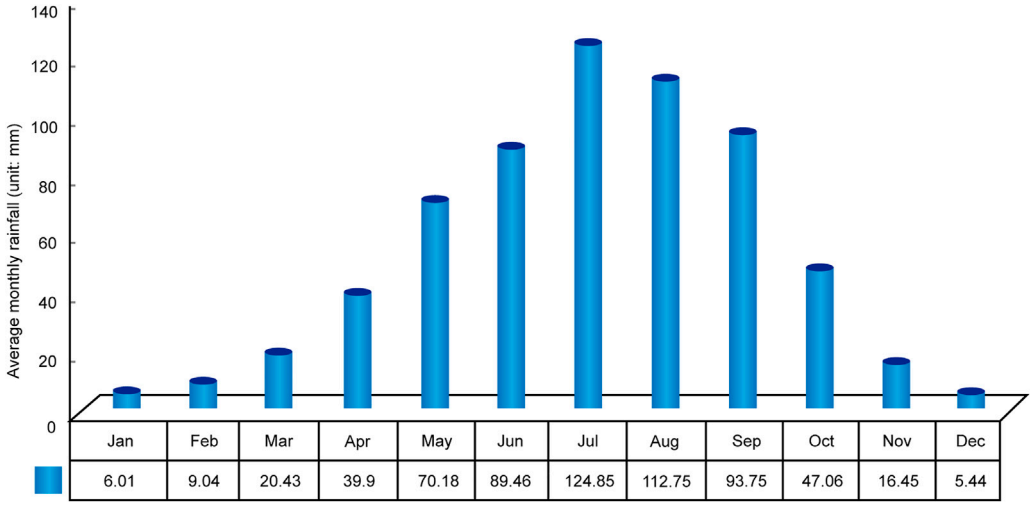

FIGURE 3 | Average water vapor flux in eastern Northwest China.

the water vapor flux divergence increases in addition to the central value and the convergence. The water vapor flux divergence reaches -1 g·cm^{-2}·hPa^{-1}·s^{-1} in May, and the water vapor convergence center is still at the junction of Gansu, Sichuan and Shanxi provinces. From June–August, the convergence area increases compared with the spring, but the convergence intensity is similar. The water vapor flux divergence is greatest in September, with a central value of -1.5 g·cm^{-2}·hPa^{-1}·s^{-1}.

The ENC is in the water vapor convergence zone, and the convergence center is at the junction of Gansu, Sichuan and Shanxi provinces.

Water Vapor Budget

The water vapor budget in four boundaries is referenced as the four sides of a rectangle shown in **Figure 5**. The monthly water vapor flux analysis shows that the water vapor in the ENC mainly originated from the southern, western, and northern boundaries. The southern boundary and the western boundary are the main water vapor input channels, while the eastern boundary is an output for water vapor. Based on analysis of the percentage water vapor flux along each boundary, the ENC is the water vapor flux output area in November, December, and January. The percentage water vapor output along the eastern boundary in winter is 51.5% in December, 53.7% in January, 52.0% in February, respectively. In other months, the percentage water vapor flux along the eastern boundary is less than 50%, indicating a net influx of water vapor in ENC. Based on analysis of the percentage water vapor fluxes along the western, southern, and northern boundaries, the proportion of water vapor flux along the northern boundary is slightly greater than 10% in December and January, whereas that for the remaining months is less than 10%. The northern boundary also had a decreasing proportion of water vapor flux from winter to summer. This indicated that NWC is located at the edge of the monsoon region, and it would not be affected by monsoons from December to March, but it is significantly affected by the northern system. In the ENC from April to September, with the increase in monsoons, the proportion of water vapor along the northern boundary decreased. The percentage monthly water vapor flux on the western border remained largely unchanged; it is approximately 25% each month, and it is 19.2% in July. The proportion of water vapor transported along the southern boundary increased to 37.9%. From August onwards, the percentage water vapor along the western boundary began to increase (to 23.7%), while it started to decrease along the southern boundary (to 31.7%). In Sep., the water vapor on the western border increased to 27.5%, while the water vapor on the southern border decreased to 31.7% (but it is still the largest source of water vapor). In October, the water vapor along the western boundary exceeded that along the southern boundary, and it decreased to 24.3% along the southern boundary. At this time, the water vapor along the northern boundary began to increase to 4.1%. In November, the water vapor along the southern boundary decreased to 17.1%. The water vapor along the western boundary decreased slowly, and the water vapor along the northern boundary increased to 8.0%.

The western and southern boundaries are the main input channels of water vapor, while the water vapor transport along the northern boundary played a complementary role. The percentage water vapor along the western boundary is stable from month to month, but the southern boundary had obvious seasonal characteristics. The output of water vapor in the ENC is characterized by seasonal differences. The eastern boundary is mainly dominated by water vapor output, and its water vapor output in winter is greater than the input. This produced drought conditions in the ENC in winter.

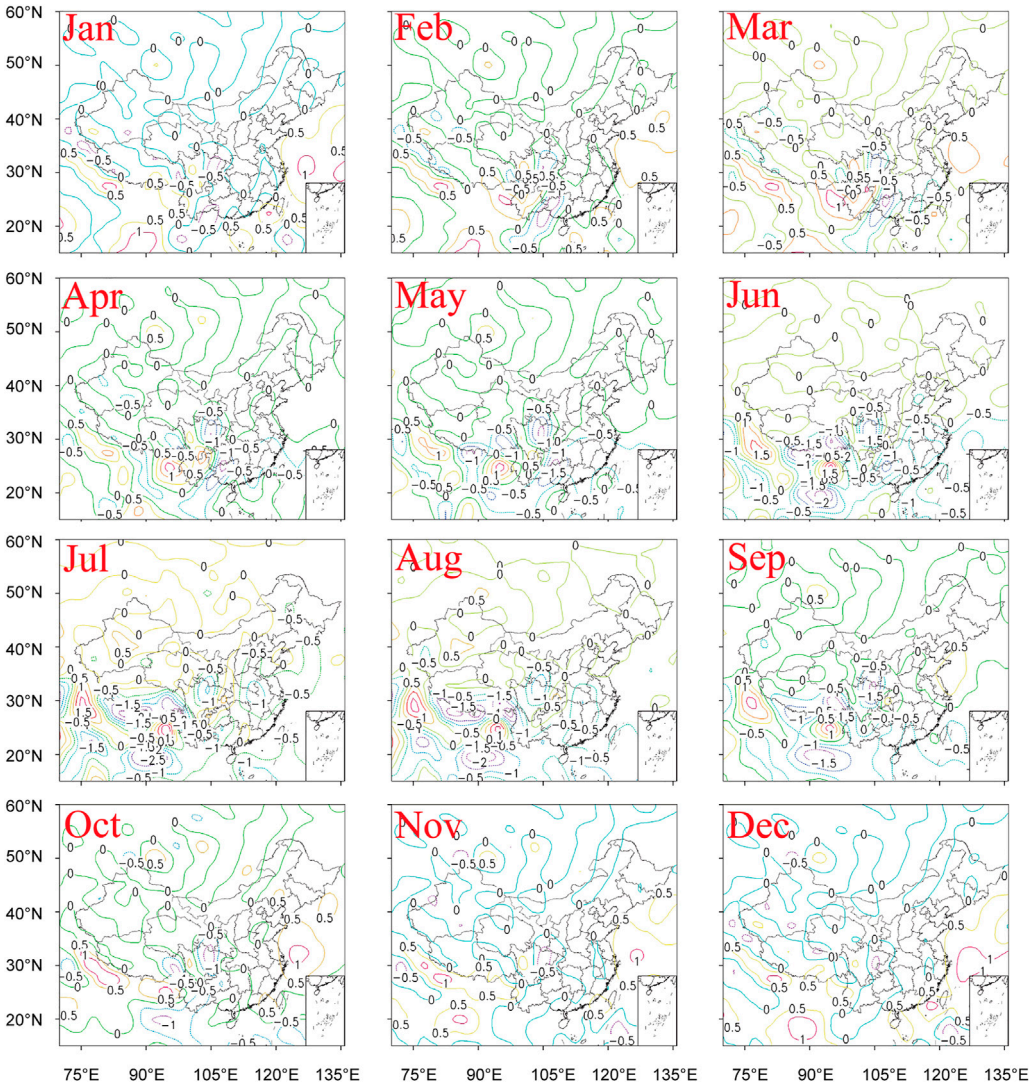

FIGURE 4 | Monthly water vapor flux divergence (Unit: $gcm^{-2}{\cdot}hPa^{-1}{\cdot}s^{-1}$).

CHARACTERISTICS OF WATER VAPOR VARIATIONS IN EXTREME DROUGHT EVENTS

Based on analysis of the water vapor budget in the ENC, the characteristics of the water vapor budget in cross-seasonal strong drought events are studied using ERA5 (0.25° × 0.25°) grid reanalysis daily data. The characteristics of the water vapor in different directions are also studied. Major extreme drought events are achieved by referencing existing research results (Ren et al., 2015).

The water vapor flux, water vapor flux divergence, and differences between the water vapor fluxes with the average value for the four boundaries of the ENC in the cross-seasonal strong drought events (**Table 1**) are calculated. **Table 1** shows that 75% of the extreme drought events had a low water vapor flux, indicating that a water vapor transport anomaly is a major cause of extreme drought. The water vapor is under weak convergence or weak divergence in all extreme drought events. With respect to the water vapor budget, the outputs of the water vapor along the eastern boundary are all positively biased and larger than the average value. This indicated that the water vapor output increased during extreme drought events. The percentage water vapor along the western boundary is reduced in most cases. The percentage change in water vapor along the southern boundary is the greatest in extreme drought events, while the proportion of water vapor on the north border increased.

The seven cases are studied by HYSPLIT, which is driven by reanalysis data (ERA5). In this paper, the moisture transport track is studied on 500 hPa, and calculate a water vapor trajectory to the ENC at intervals of 6 h. Water vapor track tracked to the first 240 h and the simulation range is (0–90°N, 0–180°E). Firstly, the water vapor trajectories contained in

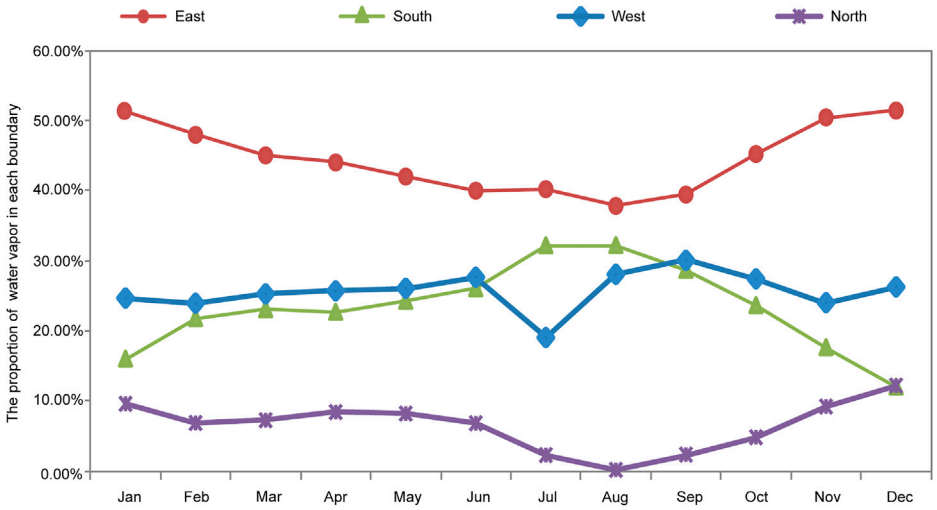

FIGURE 5 | Monthly water vapor flux percentage along the eastern, western, southern, and northern boundaries of eastern Northwest China.

TABLE 1 | The difference in the total and four boundary water vapor fluxes of the cross-seasonal strong drought events in the ENC.

Event	Beginning date	End date	Water vapor flux ($g \cdot cm^{-1} \cdot hPa^{-1} \cdot s^{-1}$)	Percentage water vapor budget difference along each boundary			
				East (%)	South	West	North (%)
1	1998–9–24	1999–5–10	4.5	2.8	−7.9%	1.8%	3.6
2	1997–4–7	1997–9–23	−24	1.2	−8.1%	−0.4%	7.3
3	1995–2–12	1995–7–24	−1.4	3.9	−9.4%	−0.7%	6.1
4	1982–3–28	1982–8–31	−4.5	4.3	−10.9%	−1.1%	4.2
5	1986–7–11	1986–11–6	−4.2	7.9	−16.6%	−1.1%	9.7
6	2004–2–14	2004–5–28	−17.7	4.8	−8.1%	−3.1%	6.5
7	2007–4–14	2007–7–17	−0.5	2.3	−7.7%	−1.7%	7.0

seven examples are tracked, and then the number of water vapor trajectories of each lattice point in monthly is calculated in the scope of study. Finally, the probability of water vapor trajectories on each lattice point in monthly is obtained. That is, the average characteristics of water vapor trajectory on cross-seasonal strong drought in monthly are obtained. Existing conclusions (**Figure 6A**) validated the following: Anomalous water vapor transport is a major cause of the cross-seasonal strong drought events. In the cross-seasonal strong drought events, water vapor output on the eastern border increased; the percentage water vapor along the western boundary is reduced in most cases; the percentage water vapor along the southern boundary is the highest in cross-seasonal strong drought events, while the proportion of water vapor on the north border increased. Concerning the conclusions mentioned above the drought analysis, it is found that when cross-seasonal drought occurs, the water origin affects the occurrence of drought, and the transport path of water vapor will affect the occurrence of cross-seasonal drought in the ENC.

The characteristics of spatial distribution on the height field on 500 hPa and the SST are synthesized according to the month of the cross-seasonal strong drought event. At the same time, the anomaly characteristics of height field and SST are also analyzed. The corresponding features of the height field (**Figure 6B**) and the SST (**Figure 6C**) show that: The ENC are controlled by Northwest airflow when the cross-seasonal strong drought occurred in the months except June, July, and August. In June, July, and August, it has a flat flow. According to the characteristics of the anomaly, the western Pacific subtropical high is found to be weak in intensity and southward in location. When this happens, it means that the ENC lacks water vapor from the south, because it lacks the dynamic conditions to transport water vapor. Abnormal SST are found mainly in the Arctic and western Pacific Ocean, when the cross-seasonal strong drought occurred. The SST is cooler the climatic average in the Arctic when the cross-seasonal strong drought occurred in February, March, April, May, and July. The SST of the Arctic is warmer, on which the cross-seasonal strong drought occurred in other months. The SST is cooler in the Western Pacific when the cross-seasonal strong drought occurred in June, July and August.

From what has been discussed above: When the cross-seasonal strong drought occurs, the water vapor transport path does not change much. The main reason is that the water vapor transport capacity is affected in the process of water vapor transport. Finally led to the occurrence and development of drought events.

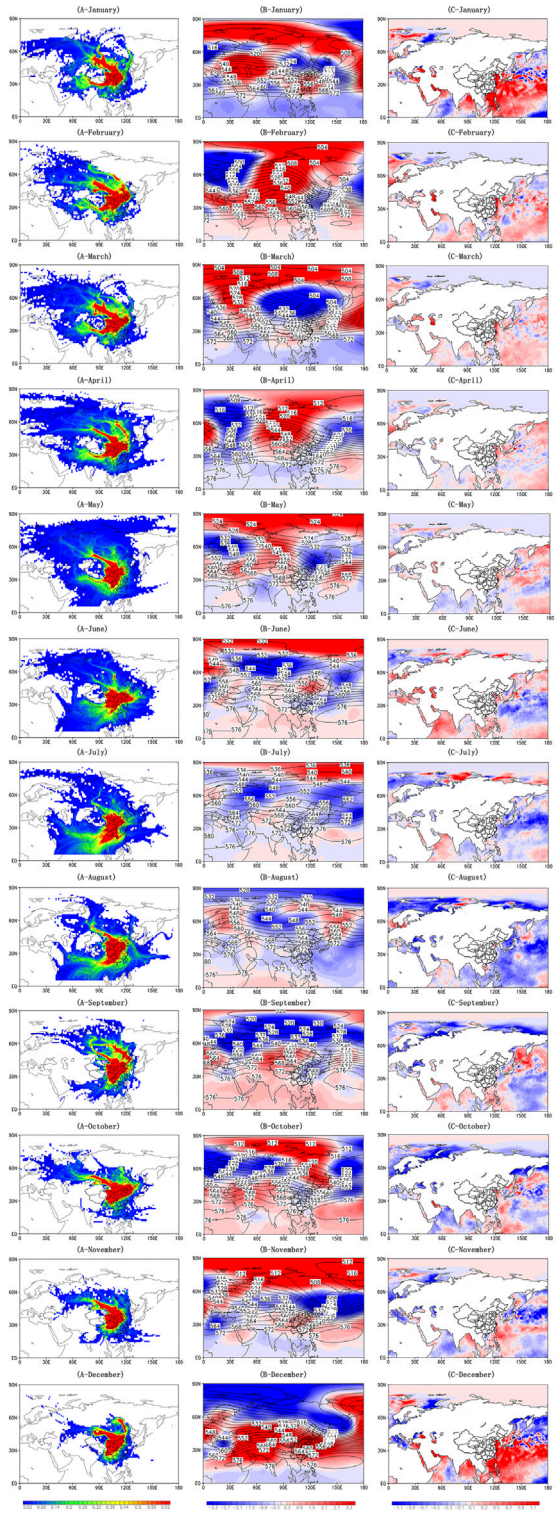

FIGURE 6 | Water vapor path of the cross-seasonal strong drought events and influencing factors **(A)**: During the month of the cross-seasonal strong drought, probability of water vapor trajectories at lattice points (Unit: %). **(B)**: The characteristics of height field on 500 hPa (Lines: The height field average, Shadow: The height field anomaly, Unit: dagpm). **(C)**: The characteristics of SST during the month of the cross-seasonal strong drought (Unit: °C).

CONCLUSION

(1) The Mediterranean Sea, Black Sea, Caspian Sea, Indian Ocean, Bay of Bengal, and South China Sea were the main sources of water vapor in the ENC, supplemented by water vapor from the mid-to high-latitude continents. From December to March, the water vapor transport from the Mediterranean Sea, Black Sea, Caspian Sea and the Indian Ocean played dominant roles, supplemented by water vapor transport in the mid-to high latitudes. In autumn, the Bay of Bengal and the South China Sea were dominant. In summer, all four water vapor sources contributed, and convergence occurred in the eastern part of the northwestern region. The transport direction of water vapor in the northwestern region was mainly to the east and north. In the water vapor flux divergence field, the eastern part of the NWC was located in the water vapor convergence zone, and the convergence center was at the junction of Gansu, Sichuan, and Shanxi provinces. The monthly water vapor flux change in the ENC was parabolic.

(2) The water vapor input in the ENC mainly originated from the western and southern borders, and the northern boundary also provided a relatively weak water vapor input. The percentage water vapor in the western boundary had little monthly change, but the southern boundary had obvious seasonal characteristics. The eastern boundary was mainly dominated by water vapor output, which exhibited seasonal differences. The water vapor output in winter was greater than the influx of water vapor, which led to winter droughts in the ENC. The input of water vapor in the western and southern borders decreased, while the output of water vapor in the eastern boundary increased. The input of water vapor along the northern boundary increased slightly. The interannual variation of the four boundaries was greatest in summer.

(3) When cross-seasonal drought occurs, the water origin affects the occurrence of drought, and the transport path of water vapor will affect the occurrence of cross-seasonal drought in the ENC.

(4) This article reveals only the causes of extreme drought in the ENC from the aspect of water vapor characteristics, but this is far from enough. In our future work, we will continue to follow this research direction to explain the problems that this article does not explain through the influence of atmospheric circulation. For example, the effects of polar vortices and the Siberian high on cross-seasonal drought events. And we will compare common drought events with cross-seasonal drought events, so that we can get the special features of cross-seasonal drought. Then we will calculate the contribution of the water vapor source for which another means to find the water vapor source site. Finally, by means of numerical simulation, the theoretical results are verified.

DATA AVAILABILITY STATEMENT

The datasets [generated/analyzed] for this study can be found in the ERA5 reanalysis data [https://cds.climate.copernicus.eu/cdsapp#!/dataset/reanalysis-era5-pressure-levels-monthly-means?tab=overview].

AUTHOR CONTRIBUTIONS

YZ was responsible for the concept and design of the work and the draft papers. KL, YR, and YL conceived the project. WS, KL, DZ, and SS were responsible for data collection. All authors contributed to the data discussion and writing of the manuscript.

FUNDING

This study was supported by the Province Natural Science Foundation of Gansu (20JR5RA118), the Major Research plan of the National Natural Science Foundation of China (91837209), National Natural Science Foundation of China (41775093), and GHSCXTD-2020-2.

ACKNOWLEDGMENTS

This work is based on the article "Water Vapor Factors Affection of Drought Events in Northwest China" published in the AMS 99th, of which is the extended and expanded work.

We thank LetPub (www.letpub.com) for its linguistic assistance during the preparation of this manuscript.

REFERENCES

Arraut, J. M., and Satyamurty, P. (2009). Precipitation and Water Vapor Transport in the Southern Hemisphere with Emphasis on the South American Region. *J. Appl. Meteorol. Climatol.* 48, 1902–1912. doi:10.1175/2009jamc2030.1

Bisselink, B., and Dolman, A. J. (2008). Precipitation Recycling: Moisture Sources over Europe Using ERA-40 Data. *J. Hydrometeorol.* 9, 1073–1083. doi:10.1175/2008jhm962.1

Chen, F., Chen, J., Huang, W., Chen, S., Huang, X., Jin, L., et al. (2019). Westerlies Asia and Monsoonal Asia: Spatiotemporal Differences in Climate Change and Possible Mechanisms on Decadal to Sub-orbital Timescales. *Earth-Science Rev.* 192, 337–354. doi:10.1016/j.earscirev.2019.03.005

Chen, C., Zhang, X., Lu, H., Jin, L., Du, Y., and Chen, F. (2021). Increasing Summer Precipitation in Arid central Asia Linked to the Weakening of the East Asian Summer Monsoon in the Recent Decades. *Int. J. Climatol.* 41, 1024–1038. doi:10.1002/joc.6727

Chen, F., Chen, J., and Huang, W. (2021). Weakened East Asian Summer Monsoon Triggers Increased Precipitation in Northwest China. *Sci. China Earth Sci.* 64, 835–837. doi:10.1007/s11430-020-9731-7

Dai, X., and Wang, P. (2020). A Review of Aridity Studies for Central Asia with Mechanism Analysis[J]. *Desert and Meteorology*. 14 (01), 1–12. doi:10.12057/j.issn.1002-0799.2020.01.001

Draper, C., and Mills, G. (2008). The atmospheric water balance over the semiarid Murray–Darling River basin. *J. Hydrometeorol.* 9, 521–534. doi:10.1175/2007jhm889.1

Guan, X., Yang, L., Zhang, Y., and Li, J. (2019). Spatial Distribution, Temporal Variation, and Transport Characteristics of Atmospheric Water Vapor over Central Asia and the Arid Region of China[J]. *Glob. Planet. Change*. 172, 159–178. doi:10.1016/j.gloplacha.2018.06.007

Knippertz, P., and Wernli, H. (2010). A Lagrangian Climatology of Tropical Moisture Exports to the Northern Hemispheric Extratropics. *J. Clim.* 23, 987–1003. doi:10.1175/2009jcli3333.1

Kwon, M., Jhun, J. G., Wang, B., An, S. I., and Kug, J. S. (2005). Decadal Change in Relationship between East Asian and WNP Summer Monsoons. *Geophys. Res. Lett.* 32, L16709. doi:10.1029/2005gl023026

Liu, J., and Stewart, R. E. (2003). Water Vapor Fluxes over the Saskatchewan River basin. *J. Hydrometeor.* 4, 944–959. doi:10.1175/1525-7541(2003)004<0944:wvfots>2.0.co;2

Ma, P. l., Yang, J. H., Lu, G. Y., Zhu, B., and Liu, W. P. (2020). The Transitional Change of Climate in the East of Northwest China. *Plateau Meteorology*, 39, 840–850. doi:10.7522/j.issn.1000-0534.2019.00093

Muñoz, E., Busalacchi, A. J., Nigam, S., and Ruiz-Barradas, A. (2008). Winter and Summer Structure of the Caribbean Low-Level Jet. *J. Clim.* 21, 1260–1276. doi:10.1175/2007jcli1855.1

Ninomiya, K. (1999). Moisture Balance over China and the South China Sea during the Summer Monsoon in 1991 in Relation to the Intense Rainfalls over China. *J. Meteorol. Soc. Jpn.* 77, 737–751. doi:10.2151/jmsj1965.77.3_737

Peng, D., and Zhou, T. (2017). Why Was the Arid and Semiarid Northwest China Getting Wetter in the Recent Decades? *J. Geophys. Res. Atmos.* 122 (17), 9060–9075. doi:10.1002/2016JD026424

Perdigón-Morales, J., Romero-Centeno, R., Ordoñez, P., Nieto, R., Gimeno, L., and Barrett, B. S. (2020). Influence of the Madden-Julian Oscillation on Moisture Transport by the Caribbean Low Level Jet during the Midsummer Drought in Mexico[J]. *Atmos. Res.* 248. doi:10.1016/j.atmosres.2020.105243

Qian, Z., Cai, Y., Song, M. H., Wu, T. W., and Zhou, J. Q. L. C. (2018). Review of Advances in Water Vapor Transport Studies of Rainstorm in Northwest China [J]. *PlateauMeteorology*. 37 (3), 577–590.

Ren, F., Gong, Z., Wang, Y., Zou, X., and Li, Y. (2015). *China's Regional Extreme Events—Droughts, Intense Precipitations, Heatwaves and Low Temperatures*. Beijing: China Meteorological Press.

Ren, G. Y., Yuan, Y. J., Liu, Y. J., Ren, Y. Y., Wang, T., and Ren, X. Y. (2016). Changes in Precipitation over Northwest China [J]. *Arid Zone Res.* 33 (01), 1–19. doi:10.13866/j.azr.2016.01.01

Ren, H., Zhang, P., Li, W., and Gao, L. (2004). Characteristics of Precipitation and Water Vapor Transport during Springtime in the Eastern Northwest China. *Acta Meteorol. Sin.* 62, 365–374. doi:10.3321/j.issn:0577-6619.2004.03.011

Roads, J. O., Chen, S. C., Guetter, A. K., and Georgakakos, K. P. (1994). Large-scale Aspects of the United States Hydrologic Cycle. *Bull. Am. Meteorol. Soc.* 75, 1589–1610. doi:10.1175/1520-0477(1994)075<1589:lsaotu>2.0.co;2

Sohn, B. J., and Park, S.-C. (2010). Strengthened Tropical Circulations in Past Three Decades Inferred from Water Vapor Transport. *J. Geophys. Res.* 115, D15112. doi:10.1029/2009jd013713

Sun, G. W. (1997). *Study on Arid Climate in Northwest China*. Beijing: China Meteorological Press, 384pp.

Wu, P., Ding, Y., Liu, Y., and Li, X. (2019). The Characteristics of Moisture Recycling and its Impact on Regional Precipitation against the Background of Climate Warming over Northwest China. *Int. J. Climatol.* 39, 5241–5255. doi:10.1002/joc.6136

Yang, J. L., Feng, J. M., Mu, J. H., Zheng, G. F., Tan, Z. Q., and Wang, S. Y. (2013). An Analysis of the Characteristics of Temporal and Spatial Variation of Seasonal Drought in the East of Northwest China[J]. *J. Glaciology Geocryology*. 35 (4), 949–958. doi:10.7522/j.issn.1000-0240.2013.0107

Zhang, Q., Lin, J., Liu, W., and Han, L. (2019). Precipitation Seesaw Phenomenon and its Formation Mechanism in the Eastern and Western Parts of Northwest China during the Flood Season. *Sci. China Earth Sci.* 62, 2083–2098. doi:10.1007/s11430-018-9357-y

Zhang, Q., Wei, J., and Tao, S. (2003). The Decadal and Interannual Variations of Drought in the Northern China and Association with the Circulations. *Climatic Environ.* 2003 (03), 307–318. doi:10.3969/j.issn.1006-9585.2003.03.005

Conflict of Interest: The authors declare that the research was conducted in the absence of any commercial or financial relationships that could be construed as a potential conflict of interest.